City Research Online

City, University of London Institutional Repository

Monitoring of the critical meniscus of very low liquid volumes using an optical fiber sensor

Leonardo Binetti, Ignacio del Villar, Kasun Dissanayake, Alicja Stankiewicz, Tong Sun, Kenneth T V Grattan, Lourdes S M Alwis

Abstract— **A novel sensing system based on single mode optical fiber in reflective configuration has been developed to measure the critical meniscus height (CMH) of low volumes of liquids, which is then used to calculate the contact angle. The sensing system has been designed especially for very low volumes of liquids (e.g. bio-liquids) and the work has demonstrated that measurements are possible with a minimum liquid volume of 5 µL. The sensing system is based on monitoring the spectral variation induced by the difference in the refractive index regions surrounding the fiber tip, at the air-liquid or liquid-liquid interfaces. From the experiments performed in water, (by immersing and extracting the fiber sensor in the liquid sample), it can be concluded that the CMH forming on the fiber decreases as the temperature increases. The change of temperature (in this experiment from 22 to 60 °C) does not influence the CMH of the sample used in the evaluation (P3 mineral oil), giving an indication of its thermal stability. In addition, a fixed fiber was used to measure the variation in the liquid level when another fiber is immersed in the liquid. The error in the liquid level obtained in the work was small, at 0.34 ± 0.04 %. Such a sensor, allowing accurate measurements with very small quantities is especially useful where liquid sample volumes are limited e.g. biologically sourced liquids or specialized, expensive industrial material in the liquid phase.**

Index Terms— **Contact angle, critical meniscus height, liquid level variation, meniscus at the interface, optic fiber sensor.**

I. INTRODUCTION

A GOOD knowledge of the spreading of a liquid on a solid is extremely important in many aspects of the use of liquid in industry or in studying biologically sourced liquids (bio-liquids). For example, it is important to have a controlled coverage of a substrate while painting, writing with ink or spraying aerosols onto a surface, to maximize quality and minimize waste. Unfortunately, liquid spreading can often be a complicated process where the presence of impurities can significantly influence the wettability and the spreading of a liquid, if these had previously been adsorbed on the surface. It is well known that when a liquid is at the interface with a solid, it forms a meniscus with a finite contact angle (CA) at the three-phase contact line (solid, liquid and air) [1]. In medical diagnostics, changes in the surface tension (ST) and the CA of biological fluids can be correlated with a range of diseases [2].

Conventional methods often require significant amounts of sample liquid (which may not always be available in the case of specific biological products). Consequently, the ability to analyze the sample and/or the accuracy of results obtained may be limited. In addition, the associated labor costs for obtaining and analyzing the sample can become prohibitively high (e.g. insulin and human blood) in associated biomedical applications. Thus, reducing the required sample size and waste in this process is extremely important [3]-[5]. Many techniques have been used to measure the height of the meniscus of a liquid formed, this bearing a direct relationship on the ST and the CA. Different examples are expensive subpixel resolution cameras, ImageJ software [6] or cathetometers. Moreover, the combination of a charged coupled device (CCD) camera with a horizontal microscope mounted together on an axial translation stage (for improved focusing) has been applied to improve the measurement of the location of the contact point of the liquid meniscus with the solid substrate. In previous experiments, complex shape probes have been immersed in the liquid to make such measurements and often the use of further theoretical analysis and/or numerical simulation is required in the accurate determination of the above-mentioned parameters from the data obtained [6]-[8].

The critical meniscus height (CMH), which is measured at the appropriate conjuncture after the meniscus breaks, has been measured in a study by Extrand *et al.* [8] and used to calculate the CA on the edge of rods attached to the beaker containing the fluid under study (thereby avoiding their floating in the liquid), of dimensions varying from 3.2 to 12.8 mm in diameter. As a result, they were able to measure the CMH just before the top of the rod was covered by the level of the liquid, as it increased. In this case, the direct measurement of the CMH was difficult to make and the result given for the CA had to be approximated [8]. One of the most used, available techniques to measure the CA is the Delta-8 Kibron multichannel tension-meter, which is based on the Wilhelmy method [9]. It uses the maximum pull force method to calculate the CA, when the ST of the liquid is known. This technique uses a 0.5 mm diameter probe and needs a sample volume of only 50 µL [10].

Optical fiber sensors have also been demonstrated to be extremely attractive for a wide range of measurements because of features such as their immunity to electromagnetic interference, resistance to corrosive or biohazardous chemicals

I. del Villar is with the University of Navarra (e-mail: ignacio.delvillar@unavarra.es)

K. Dissanayake, T. Sun, K. T. V. Grattan are with the City, University of London, (e-mail: Kasun.Dissanayake@city.ac.uk, T.Sun@city.ac.uk, K.T.V.Grattan@city.ac.uk)

and their small size [11], [12]. This small size feature, taking advantage of the diameter of a standard single mode fiber (SMF) being typically 125 µm, is especially attractive in chemical detection applications where, as will be shown, a much smaller sample volume can be used due to the small size optical fiber. Optical fiber methods are very effective when measuring refractive index (RI), a measurement which is important in many chemical and biological applications [13]. Further, different techniques have been used to measure the CA of a liquid by immersing an optical fiber in a sample of the liquid. For example, Zhou *et al.* [14] and Márquez-Cruz *et al.* [15] have measured the dynamic and the static CA, respectively, using a fiber probe when it was (vertically) immersed in the test liquid. Shen *et al.* [16], and Liu *et al.* [17] have described an alternative technique where a tilted fiber Bragg grating was immersed horizontally into the liquid. In that approach, the length of the liquid film was set to be 18 mm so that the fiber was completely wet, allowing the detection of the variation in signal when the fiber was in air. By placing the fiber perpendicular to the surface of the liquid, only the 125 µm diameter of the fiber tip is made to wet and thus the liquid sample size needed is reduced. This is more convenient to use in practical applications, since it functions as an immersion probe. In the above-mentioned methods, a CCD camera or a telescope-goniometer were used to capture the profile of the liquid surface around the interface with the fiber. The main drawbacks of these techniques is that the camera/telescope is tilted down (at 1-2 degrees from the horizon of the liquid sample), there is the need for a strong background light and there is an increase in the complexity of the approach to make the reading, due to the cylindrical shape and small size of the optical fiber used. In addition, particular skill is needed by the experimentalist to use the technique well and thus create reproducible and accurate results [18], [19].

However, from a review of the literature undertaken, it would appear that creating a sensor based on monitoring the CMH by using an optical fiber sensor emerging vertically from the air/liquid and from the liquid/liquid interfaces and then calculating the CA (all without the use of cameras), is innovative and this approach has not been investigated in any detail. Thus, the background work done by the authors suggests that a simple and precise optical fiber-based sensor to measure the CMH of a liquid by detecting the variation in the surrounding RI at the tip of a bare fiber could be developed. As a result, a small diameter probe, based on using a 125 µm diameter optical fiber has been used in this work. The reason for that is due to the fact that Sauer *et al.* [20] demonstrated that the small diameter fiber used facilitates the rapid equilibration of the meniscus on a stationary fiber, resulting in a high level of measurement of accuracy and reproducibility. In addition, the silica glass optical fiber that forms the basis of the sensor has the advantage of chemical inertness compared to the use of polymeric fibers (which are more easily damaged by aggressive fluids) for similar applications, e.g. for monitoring caustic or acidic liquids. An important feature of the sensor is that the required volume of the liquid sample needed (into which the fiber tip is immersed) can be small and thus limited volume sample sizes can be used, which is important, for example, when expensive or scarce samples require analysis. A further advantage is that the sensor approach is non-destructive:

samples can be reclaimed after the measurement has been made and used for other types of analysis as the optical fiber probe does not contaminate the sample.

II. Methodology

A. Chemicals

The following chemicals used were of analytical grade and used as supplied, with no other purifications being carried out. Isopropanol at 70% in water (IPA) was purchased from Sigma Aldrich UK. Extra pure, deionized water was obtained from Acros Organics. P3 mineral oil (used as an exemplar fluid for the measurements made in this work) with a density of 870 kg/m^3 at 20 °C, and a high operating temperature up to 95 °C, was purchased from Pfeiffer Vacuum. The ITU G.652.D pigtail optical fiber with standard connector type SC has core and cladding diameters of 9 µm and 125 µm, respectively.

B. Experimental setup for CMH sensor

The fiber sensor system developed in this work is comprised of an optical sensor interrogator unit (Micron Optic sm125 – with a low noise feature with fiber Fabry-Perot tunable filter technology), which is connected to a computer to read out the variations observed in the reflected optical spectrum. The benefits of using the interrogator unit include allowing the continuous monitoring of the optical power variation, together with the variation of the amplitude of the interference signal. To address any measurement inaccuracies that could occur from the variation on the light source optical power [21], the detection of the reflected optical power was conducted three hours after turning on the interrogator, to guarantee the stability of the source and optical power transmitted to the fiber. One end of the SMF was connected to the interrogator, while the other was stripped of its polymeric dual acrylate coating and cleaved at 90°. This cleaved end was then placed in a test chamber and attached to a tensile machine (Lloyd Instruments QA LRX 05), as shown in Fig. 1, to apply a known, and a reproducible motion. A major advantage of using this tensile machine is that its speed can easily be controlled, and it has been configured to operate at very low speeds (down to 0.1 mm/min) so that any vibrations reaching the test chamber would be minimized.

The test chamber includes a plastic shield, which provides protection to the fiber from stray air currents, as is shown in Fig. 2. In addition, the cleaved end of the fiber was attached to a PVC support, which was then connected to a metallic bridge to minimize any vibration reaching the fiber. In addition, the liquid solution was put into a cylindrical Pyrex glass beaker that was mounted on a neoprene rubber base, to avoid any vibration from the movable arm of the tensile machine interfering with the measurement. The cylindrical fiber and the cylindrical beaker were positioned coaxially, to create an axisymmetric system. The liquid solution was allowed to move upwards and downwards so that the cleaved fiber could be submerged in and then extracted from the liquid sample, as required. In addition, vibrations on the fiber and thus potential errors in the measurement were reduced by moving the solution instead of the fiber, a technique demonstrated by Champmartin *et al.* [6].

In order to measure the CMH, the following procedure was undertaken. Prior to making a measurement with a liquid

sample, the fiber was first cleaned with IPA and deionized water and then dried. Then, the power reflected from the optical fiber tip, surrounded by air (which has a RI, n_{air}, of ~1.0) in the wavelength range from 1520 to1580 nm, was recorded. The cleaved end of the optical fiber was then submerged in the liquid, which was allowed to move upwards (at a speed of 0.1 mm/min) and then stopped when a variation in the reflected power of the fiber was detected, this being due to the contact of the cleaved fiber with the liquid. The optical fiber has, at this stage, reached the undisturbed surface of the liquid and the meniscus forms around the fiber, wetting the fiber tip. Following this, the reflected power was recorded, and the solution was then further made to move downwards with the same controlled speed. The reflected power remains unchanged until the meniscus breaks – here the fiber is in contact with the liquid until the meniscus rupture occurred. The process, as a series of steps is illustrated in Fig. 3. The height of the meniscus was then observed from the recording of the time needed for the fiber to register a different reflected power, comparing that with the value obtained when the fiber was in contact with the liquid (i.e. the time it takes to transit from the stage shown in Fig. 3(b) to that in Fig. 3(d)). Each measurement of the CMH was repeated three times, to evaluate the repeatability of the measurement and the above process was then monitored with changing speeds and temperatures, in order to create a full characterization of the measurement system. The critical height of the meniscus after which it breaks (h), the receding CA (ϑ) and angle φ (given by π/2 – ϑ), are represented in Fig. 3(e). The two liquid samples selected here – oil and water – have different values of ST (approximately 28 mN/m [22] and 72 mN/m [23], respectively): this being a range typical of most liquids that would be studied [24].
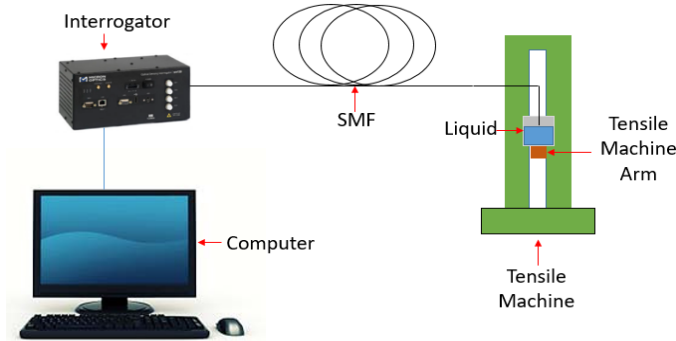

Fig. 1. The measurement setup with the optical interrogator and the tensile machine arm used to move the liquid solution.
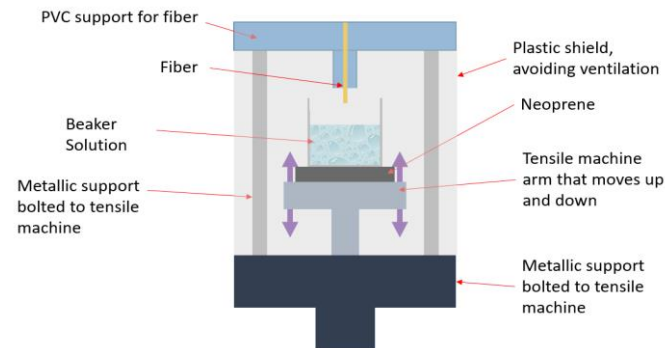

Fig. 2. Illustration of the liquid being moved up and down while the fiber is attached to the metallic bridge via a PVC support.
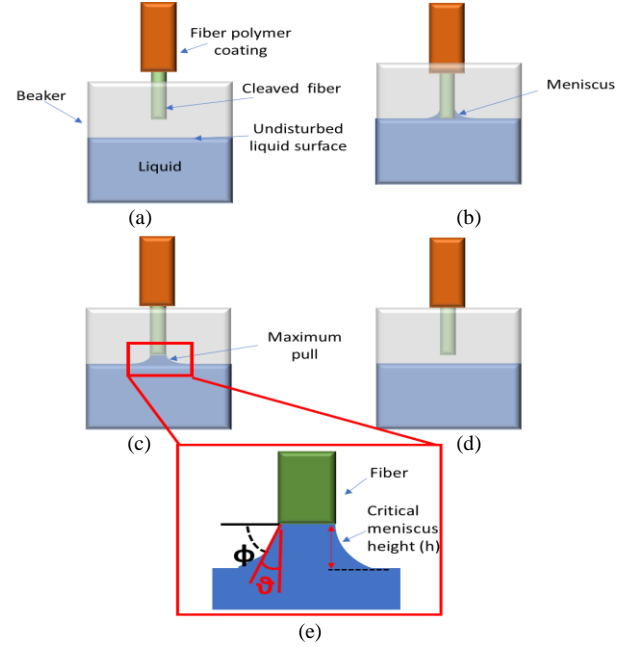

Fig. 3. Fiber immersion and extraction stages: (a) in air, (b) in the liquid while the meniscus forms, (c) when the maximum pull is reached, (d) fiber out of the solution, (e) closer examination of the CMH (*h*) and the receding CA *ϑ*. Measurements were taken when fiber is held in place while the beaker is moved up and down.

C. Selection of the diameter of the beaker.

Next, the CMH measurement of the liquid was performed to investigate the effect of the different diameters of the beakers used, in order to determine the optimum diameter (following which the measurement of the CMH remains constant). The reason for this is that the wettability of the liquid increases as the diameter of the container decreases, which leads to capillary pressure (through the Young-Laplace equation). It is the difference between the ambient pressure and the pressure of the column of liquid which is directly proportional to the liquid ST [25]. For this reason, Pyrex™ glass beakers of different diameters, ranging between 5.4 to 56.6 mm were used in the experiments.

White *et al.* [26] have derived the equation for the CMH for a rod, as follows:

$$h = \left[2\left(\frac{\gamma}{\rho g}\right)(1 - sin\varphi)\right]^{\frac{1}{2}}\left[1 + \left(\frac{\gamma}{\rho g}\right)^{\frac{1}{2}}\frac{1}{R}\right]^{-\frac{1}{2}} \qquad (1)$$

where γ is the ST of the liquid, R is the radius of the fiber, ρ the density of the liquid and g the acceleration due to gravity. In this case, the angle monitored is the receding CA (ϑ), given by (π/2 – φ) from Fig. 3(e). For a small diameter fiber, the equation describing ϑ can be given as follows:

$$\theta = \cos^{-1}\left(1 - \frac{h^2(1+\frac{1}{R}\left(\frac{\gamma}{\rho g}\right)^{\frac{1}{2}})}{2\frac{\gamma}{\rho g}}\right) \qquad (2)$$

D. Investigation of the CMH with different liquid volumes.

Once the appropriate diameter of the beaker has been selected, using the approach described above in Section C, the CMH measurement was conducted with different volumes of liquid, with the aim of understanding better what volume of liquid sample presents a constant value of CMH. The volumes of the liquid sample under analysis ranged from 5 µL to 1 mL and, as demonstrated later in the results section, it was shown that the CMH decreased as the volume decreased.

E. Experimental setup for measuring CMH at the interface between two liquids.

The CMH at the interface between two liquids can be determined readily by using water and oil as the test liquid samples, as these two liquids possess significantly different density and RI values. The RI of oil (n_{oil}) and water (n_{water}) were calibrated for the experiment by using a 30GS refractometer (from Mettler Toledo Inc.), operating at a wavelength of 589.3 nm. The results obtained for the RI were 1.477 and 1.333, respectively. In view of the difference in the RI of the two liquids, the reflected power of the optical fiber was recorded individually for both the oil and the water samples. In addition, the CMH at the interface was determined by measuring the time needed to break the meniscus at the interface, by monitoring the changes in the reflected power, as shown in Fig 4.
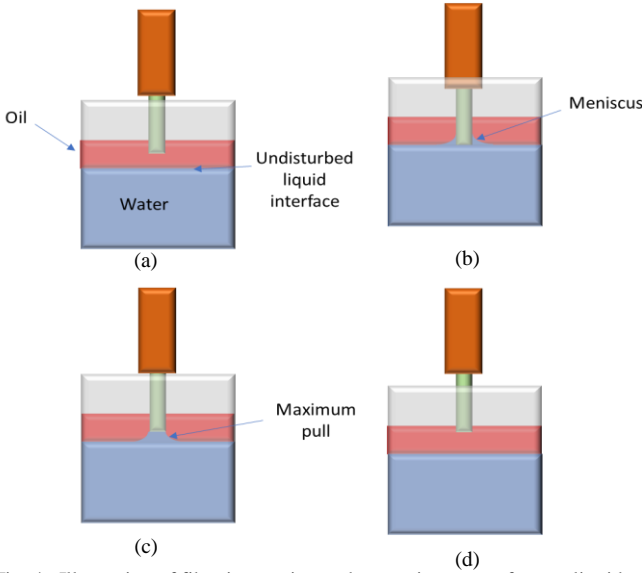

Fig. 4. Illustration of fiber immersion and extraction stages for two liquids: (a) in oil, (b) in water while the meniscus forms, (c) the maximum pull is reached, (d) again in oil. During measurements, the fiber is held in place with the beaker moving up and downwards.

F. Experimental setup for interface thickness measurement

The measurement of the interface thickness between the oil and the water liquid samples was determined by recording the increase in the mean value of the reflected power observed, up to the point where the reflected power achieves the expected value for the water sample. The interface thickness was calculated by recording the reflected power when moving the beaker at a constant speed of 0.1 mm/min and noting that the measurement was complete once the fiber reached the water level point. The experiment was performed both before and

after a centrifugation process was carried out to remove any air trapped between the two liquids, at 10000 rpm for 5 min using a Sorvall RC 6+ centrifuge.

G. Correction of liquid level

The liquid level is affected when a solid is placed in contact with a liquid solution and a decrease in the liquid level would be expected when the meniscus has formed [6]. Therefore, the height of the liquid surface that is monitored must be corrected accordingly. In order to correct this problem, the liquid level variation was measured using two fibers. Thus one of the fibers was fixed to the glass beaker at 0.2 mm distance from the liquid surface to record the reflected power variation before and after the other fiber comes in contact with the liquid, which was achieved by moving the beaker (containing the liquid) upwards, as illustrated schematically in Fig. 5.
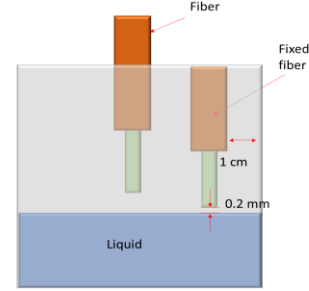

Fig. 5. Optical fiber fixed to the beaker registers the variation of the liquid level while the beaker moves upward allowing the other fiber to be immersed in the liquid.

III. RESULTS AND DISCUSSION

A. Investigation of beaker diameter.

As stated in Section II, in order to select the most appropriate beaker dimension, the CMH measurement was conducted with a wide variety of different beaker sizes, these ranging from 5.4 to 56.6 mm, and allowing the two properties of the two different liquids to be measured with the same set-up and beaker size. Repeated measurements were carried out for two different liquid samples –water and oil – at 22 °C and a fixed speed of 0.1 mm/min. Each beaker was filled with the liquid, up to 75 % of its full capacity. Prior to any test being undertaken, the reflected power values in air, water and oil were recorded, as shown in Fig. 6. Fig. 7 shows the results and represents the variation of the CMH for water (when in contact with the optical fiber) with different diameters of the beaker being used. The value of the CMH was approximately constant when the diameter of the beaker used exceeded 20 mm, which demonstrates that the capillary pressure does not change any further, in agreement with the observations of Selley [25]. In addition, no appreciable variation was seen when water was substituted for oil in measurements made using the range of beaker diameters selected. This is explained by the fact that the oil has a lower ST than water at this room temperature. Hence, a relatively smaller beaker diameter chosen from the selected range should be used for oil and further investigation of this effect is beyond the scope of this paper.
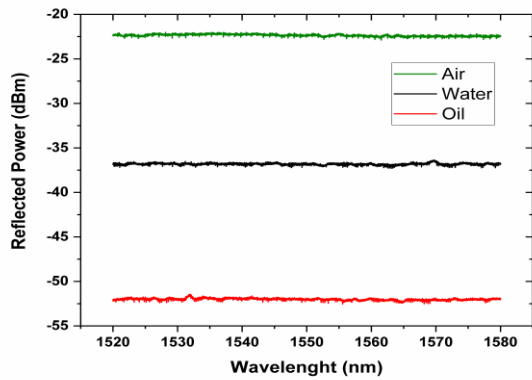
Fig. 6. Representation of the different reflection spectra from the optical fiber tip for air, water, and oil.
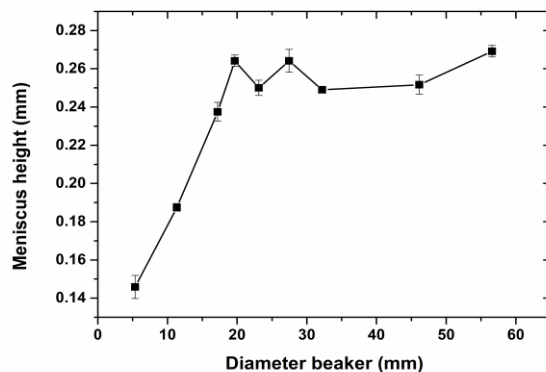

Fig. 7. Variation of CMH (at a fixed movement speed) for water contained in different diameters of beakers (at a fixed temperature).

As a result, the smallest beaker diameter, with a size of ~20 mm, was chosen for further analysis to be undertaken, with the aim of evaluating the extent to which the amount of liquid sample needed could be decreased. This value chosen was the first diameter of beaker available, after which the CMH remained constant. The value of the CA calculated for water, using (2) was 37.86 ± 0.42° at a CMH of 0.264 ± 0.003 mm. The literature data available to undertake a comparison are limited but Sklodowaka *et al.* measured the CA of silica to be 38.9 ± 0.84° [27] which is in good agreement. A further important conclusion is that it was possible to measure the CMH of the liquid with the use of a very small beaker diameter, which then supports the use of small volume liquid samples in the measurement.

B. CMH and volume of liquid.

Once the beaker diameter was selected (based on the above results), the measurement of the CMH as a function of the liquid volume was conducted, using both water and oil (at 22 °C) as the sample media. Results obtained from these tests are shown in Fig. 8, showing that an effective measurement of the CMH of water could be performed with the use of a very small volume of the liquid, i.e. 5 μL and taking advantage of the small diameter of the fiber used. The importance of this result is that the volume of liquid required is much less than is needed for typical commercially available techniques, such as the Delta-8 (Kibron), which requires 50 μL – this giving a reduction in the liquid sample size by an order of magnitude.

The second important result, represented by the black line (left hand side) in Fig. 8, is that the value of the CMH remains stable when a droplet of 100 μL, or above, is evaluated. This means that the droplet diameter has become sufficiently large and the fiber tip sees the droplet as a flat surface. Thus, at this stage the CMH is not primarily influenced by the radius of the droplet but by the radius of curvature of the meniscus forming on the fiber, as described by the Young-Laplace equation. This equation gives a result for the capillary pressure which is inversely proportional to the surface curvature of liquid [28], which also depends on the sample volume and the surface area [29]. A figure similar to Fig. 8 could be obtained for an oil sample, but it is not shown since no variation of the CMH was detected for the liquid volume range selected. In this case, the meniscus height had a constant value of 0.24 ± 0.01 mm throughout the liquid volume range selected, which was from 5 to 1000 μL. The reason for this is that the oil was totally spread out on the Pyrex beaker glass surface, so that the droplet is seen as 'flat'.

A variation of the CMH in the liquid volume region between the black and red lines is present, as illustrated in Fig. 8. In this case, the liquid has either a concave (right hand side of the figure) or a convex shape (left hand side), depending respectively on whether or not the liquid makes contact with the beaker wall. The CMH variation between the black and red line, at the plateau (ΔCMH shown on the figure), is 14.1 ± 4.1 μm. This variation arises due to the fact that the CA of the liquid droplet (with respect to the surface of the beaker) is not $\pi/2$ (in the convex shape case, CA convex), and also the CA between the liquid and the wall of the beaker is not $\pi/2$[19] (in the concave case CA concave), represented in Fig. 8.

In light of these results, a 0.5 mL solution was poured into a 20 mm diameter beaker, since it is the minimum beyond which the value of the CMH does not change (for water) and this arrangement is used for the next set of experiments carried out and discussed below.
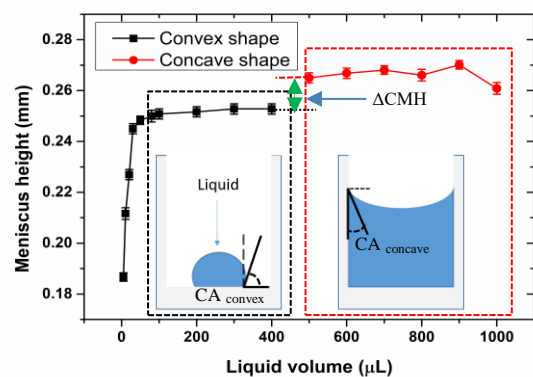

Fig. 8. Variation of CMH at a fixed speed for different volumes of water.

C. CMH measurement of water and oil

In light of the previous results, repeated measurements were carried out in water and in oil, at different temperatures, using a beaker of ~20 mm diameter and a 0.5 mL solution, in order to characterize the CMH measurement. The variations in the CMH of water, as shown in Fig. 9, obtained when the fiber withdrawal speed was 0.1 mm/min and the temperature changed from 22 °C to 60 °C. It was clearly demonstrated through this that the

CMH varied with temperature, which is due to the state of the hydrogen bonding in water, which consequently becomes weaker [30]. Different speeds of extracting the fiber from the liquid were investigated (up to 2 mm/min) and no appreciable CMH changes were detected, a similar result to that demonstrated by Extrand *et al.* [8]. Hence, it is possible to conclude that the CMH decreases with the increase of temperature over the range shown, a result that is important for monitoring of low volume sample bio-liquids.
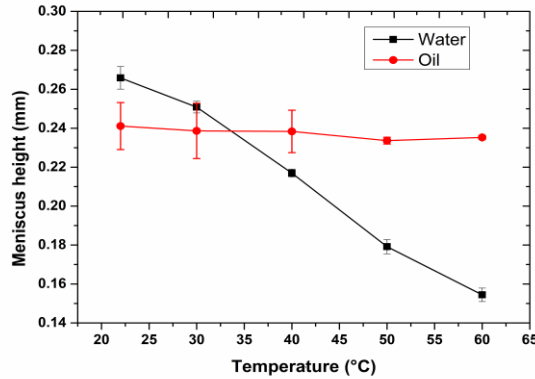

Fig. 9. Variation of the CMH with temperature, at a fixed fiber withdrawal speed, for both water (black) and oil (red) samples.

Investigating this situation further, the CMH of the oil sample was measured over the range between room temperature and 60 °C. As can be seen from Fig. 9, the CMH (for oil) does not change (within experimental error) with temperature, confirming that these properties for oil are stable over this temperature range.

D. Interface CMH measurement

The measurement of the CMH at the interface between oil and water sample was performed, with a fiber withdrawal speed of 0.1 mm/min, carrying out the tests at different temperatures, with the results as shown in Fig. 10. It can be seen that the CMH at the interface decreases as the temperature increases, this being mainly due to the fact that the CMH of water decreases with an increase in temperature, as shown in Fig. 9. It is also interesting to observe that the rate of decrease is lower than that for pure water, possibly due to the presence of oil.
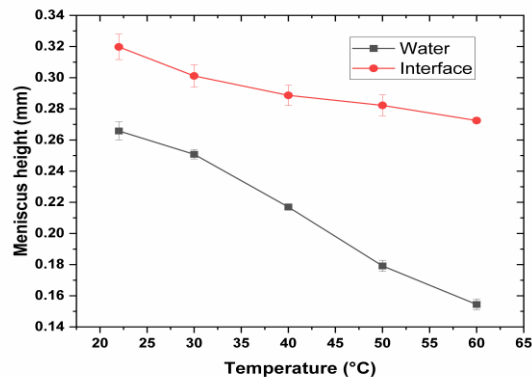

Fig. 10. Variation of the CMH at the interface between the two liquids (oil and water) as a function of temperature variation, at a fixed speed fiber withdrawal speed, compared to water.

E. Presence of air layer at the interface

In the next experiment carried out, when the beaker containing the two liquids was moved upwards toward the fiber (as shown in Fig. 4(a)), the power reflected by the fiber initially experiences a variation due to the presence of the oil layer. Just before the fiber reaches the water, the average value of the reflected power increases (blue and magenta lines in Fig. 11(a)). The opposite case (reflected power decreases) occurs when the fiber reaches the water or oil from the 'air side' (black and red lines). The reason for this occurring is due to the fact that, contrary to the situation for air, n_{oil} is higher than n_{water}.

A further investigation showed that the value of the average reflected power measured when the fiber was in contact with water is ~ -36.8 dBm illustrated in Fig. 11(a) at 0.00 µm distance. At 0.01 µm distance from water, the average reflected power, the blue curve in Fig. 11(a), increases up to ~-35.6 dBm. However, after the sample is centrifuged, the average reflected power (magenta curve) was ~ -40 dBm, at a position of 0.01 µm. This value does not exceed the average reflected power for the water sample, which is possibly due to the fact that some small air bubbles are likely present between the oil and water (possibly due to the high absolute viscosity of the oil used (82.6 mPa·s), trapping small air bubbles between the oil and water samples [31]) – this effect was then removed following the centrifugation which was carried out. In addition, the statistical error bar for the points on Fig. 11(a) is small, (~0.2 dBm) hence it is not shown. The spectrum of the reflected power is shown in Fig. 11(b) for several different situations: when the fiber is in air, in water, in oil and at the interface between oil and water, at 0.01 mm distance from the water, both before and after centrifugation. The variation of the air layer thickness at the interface between the oil and water, for a situation where the temperature is varying and at a fixed fiber immersion speed of 0.1 mm/min, is represented in Fig. 12. It is clear from this figure that the thickness of the layer decreases with the increase in temperature, which provides thermal energy to the small air bubbles to allow them to escape from this region, a result which implies that an air gap is present at the interface if the sample is not centrifuged.
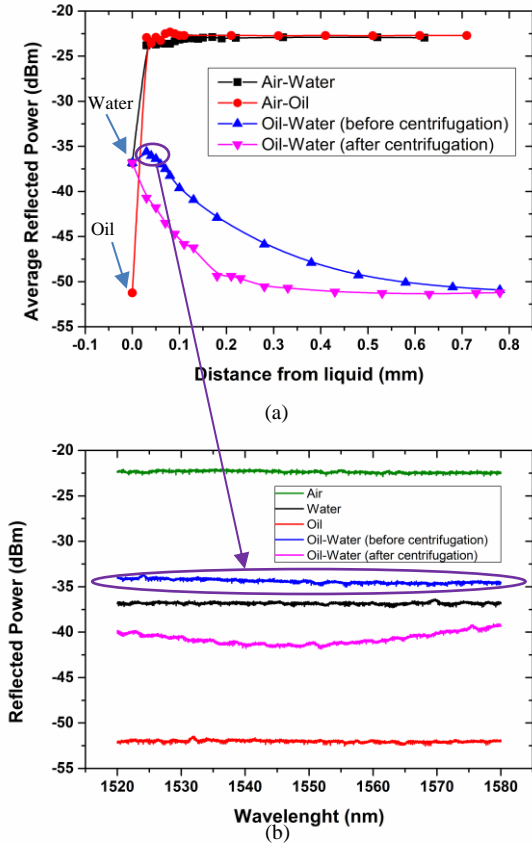
Fig. 11. Representation of (a) the average reflected power from air-water, air-oil, and oil-water, before and after centrifugation and (b) the different reflection spectra for air, water, oil and the interface between oil and water (before and after centrifugation, at 0.01 mm distance from the water surface).
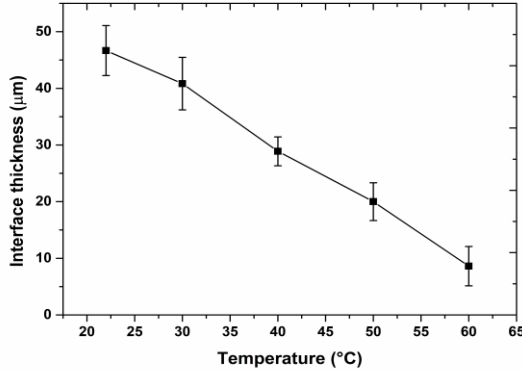

Fig. 12 Variation of the air layer thickness at the interface between oil and water, for varying temperatures, at a fixed fiber immersion speed of 0.1 mm/min.

F. Correction liquid level

As discussed in the Section II (subsection G), in order to measure the liquid correction level, two cleaved fibers were used: a fiber that will be immersed in water and a fiber fixed to the beaker, using the set up shown in Fig. 5. Water was chosen for this experiment since it presents a CMH that is higher than that of oil, at the temperature of the experiment, thus it shows the highest variation of the liquid level. It could be noted that the amplitude of the interference pattern observed in the reflected spectrum increased as the liquid surface became closer

to the first fiber, moving from 0.38 to 0.03 mm, as shown in Fig. 13. The spectrum was then recorded once the liquid stopped moving, at different distances from the tip of the first fiber. The reflection spectra observed and shown in Fig. 13 give evidence of these oscillations occurring due to the interferometric cavity created by the air gap between the water surface and the fiber tip. The amplitude of these oscillations can be seen in Fig. 14, where an exponential increase can be observed at distances close to the surface of the water. The same behavior is present for oil, showing a clearer exponential curve performance than for water because of the higher refractive index of oil (compared to water), which increases the effect seen in the interferometer. However, the behavior is quite different at the interface between oil and water. In this case, contrary to the situation with the air cavity, an oil cavity (which has a refractive index lower than the silica optical fiber, but higher than that of water) is now formed between the silica optical fiber and the water. Moving from long to short distances, the increase in the amplitude of these oscillations reached a maximum, and after that there is a progressive decrease of the amplitude, to a point where the fiber reaches the water. This position of this maximum is not an indication of the fiber entering the air cavity which is analyzed in Fig. 12, because at 22 ºC the thickness of this cavity is around 50 μm, far from the 200 μm and the 600 μm maxima observed in Fig. 14, for the centrifuged and non-centrifuged cases respectively. It is, rather, a consequence of the effect of the air bubbles at the oil-water interface [31], which induces a different scattering of light at the surface and hence a different amplitude in the oscillations. The statistical error seen is negligible (and thus not indicated on the graph). The point at distance 'zero' is that point where the liquid surface reaches the fiber and the meniscus forms.
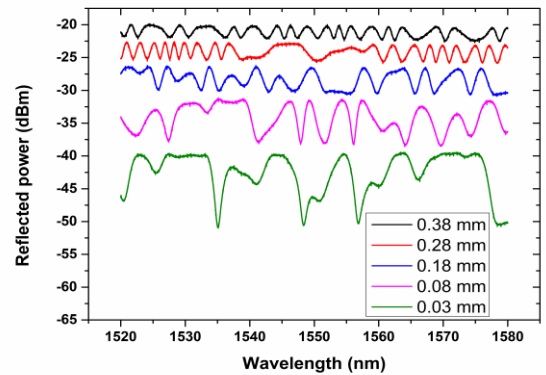

Fig. 13. Increase of the amplitude of the oscillations in the reflection spectra, as the distance between the fiber tip and the water surface decreases from 0.38 to 0.03 mm.
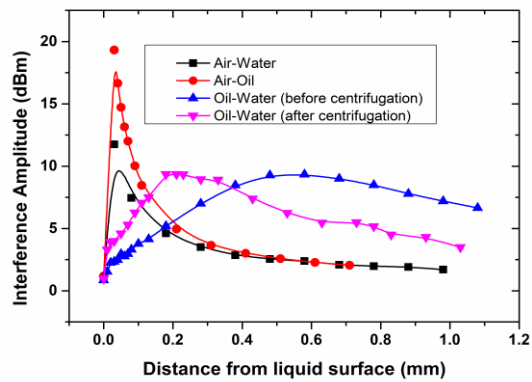
Fig. 14. Increase of the amplitude of the oscillation in the reflection spectrum as the liquid surface (water and oil) reaching the fiber. Decrease of the amplitude in oil-water before and after centrifugation. Liquid level at 0.0 mm.

One fiber was fixed at 0.2 mm from the water level to register the variation of the interference amplitude both before and after the liquid surface reached the other fiber, as shown in Fig. 5. In this case, the amplitude of the interference pattern seen before and after the liquid reached the fiber is shown in Fig. 15. The variation in interference amplitude is 0.34 ± 0.04 %, which indicates that the contribution of the liquid level variation was very small and has a negligible effect on the results shown.
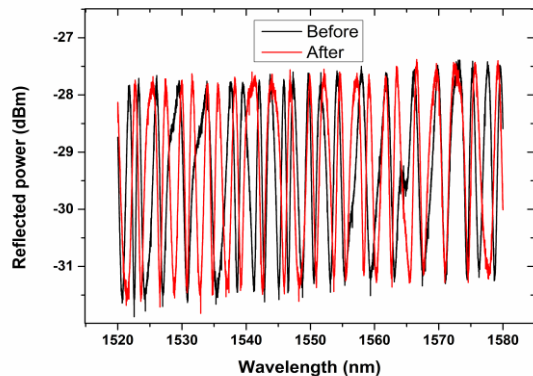

Fig. 15. Variation of the amplitude of the oscillations measured by the fixed fiber before and after the liquid reaches the first fiber, forming the meniscus.

IV. CONCLUSION

The results presented in this paper demonstrates that a single mode silica optical fiber-based sensor system can be used to measure the CMH of a liquid, with high precision and that it is possible to decrease the volume of liquid needed for the analysis, i.e. to 5 µL. The CMH of water decreases with temperature and further, the stability of the mineral oil P3 used has also been investigated as a function of temperature, to characterize the process discussed. The presence of an air bubble layer is likely to be between the oil and the water samples used. Finally, the work has shown that the single mode silica fiber does not influence the reading of the CMH since it does not require a correction of the liquid level. The study has shown that the system can be used as an accurate and easy-to-implement tool for measuring the properties of liquids. Furthermore, and most importantly, the proposed system allows a very small volume to be used for the measurement of

wettability in medical diagnostics, while changes in the surface tension (ST) and the CA of biological fluids can, as has been discussed in the literature, be correlated with a range of diseases. This approach shows advantages over conventional methods in not requiring significant amounts of sample liquid, which often are not available or convenient to extract from the patient, where otherwise the accuracy of results obtained would be limited. Work is currently ongoing to examine a wider range of fluids using this technique.

REFERENCES

[1] A. Cazabat, "How does a droplet spread ?," *Contempoary Physics*, vol. 28, no. 4, pp. 347–364, Aug. 1987.
[2] H. N. Harkins, W. D. Harkins, "The surface tension of blood serum, and the determination of the surface tension of biological fluids," *Journal of Clinical Investigation*, vol. 7, no. 2, pp. 263–281, Jan. 1929.
[3] J. H Simons, W. H. Wilson, "Surface tension and viscosity of liquids," *The journal of chemical physics*, vol. 23, no. 4, pp. 613–617, Jul. 1955.
[4] M. Vaccari, T. Tudor, A. Perteghella, "Costs associated with the management of waste from healthcare facilities: An analysis at national and site level," *Waste Management and Research*, vol 36, no. 1, pp. 39–47, Oct. 2018.
[5] E Kachooei, A. A. Moosavi-Movahedi, F. Khodagholi, et al., "Oligomeric forms of insulin amyloid aggregation disrupt outgrowth and complexity of neuron-like PC12 cells," *Plos One*, vol. 7, no. 7, Jul. 2012.
[6] S. Champmartin, A. Ambari, and J. Y. Le Pommelec, "New procedure to measure simultaneously the surface tension and contact angle," *Review Scientific Instruments*, vol. 87, no. 5, pp. 0–7, May 2016.
[7] A. Kalantarian, R. David, J. Chen, and A. W. Neumann, "Simultaneous measurement of contact angle and surface tension using axisymmetric drop-shape analysis-no apex (ADSA-NA)," *Langmuir*, vol. 27, no. 7, pp. 3485–3495, Feb. 2011.
[8] C. W. Extrand and S. I. Moon, "Critical meniscus height of liquids at the circular edge of cylindrical rods and disks," *Langmuir*, vol. 25, no. 2, pp. 992–996, Dec. 2009.
[9] G. Dour, A. Hamasaiid, "Wilhelmy surface tension measurement applied to metallic alloys - static and dynamic measurements in molten and semi-solid states," *Journal of Composite Materials*, vol. 48, no. 3, pp. 1–18, Aug. 2014.
[10] C. Johans, I. Palonen, P. Suomalainen, P. Kinnunen, "Making surface tension measurement a practical utility for modern industrial RD," *American Laboratory,* vol. 37, no. 25, pp. 0–14, Dec. 2005.
[11] Y. Tian , B. Xu, Y. Chen, C. Duan, T. Tan et al., "Liquid surface tension and refractive index sensor based on a side-hole fiber bragg grating," *IEEE Photonics Technology Letters*, vol. 31, no. 12, pp. 947–950, June 2019.
[12] T. H. Nguyen, T. Venugopalan, T. Sun, and K. T. V. Grattan, "Intrinsic Fiber Optic pH Sensor for Measurement of pH Values in the Range of 0.5-6," *IEEE Sensors Journal*, vol. 16, no. 4, pp. 881–887, Feb. 2016.
[13] A. Urrutia, I. Del Villar, P. Zubiate, and C. R. Zamarreño, "A Comprehensive Review of Optical Fiber Refractometers: Toward a Standard Comparative Criterion," *Laser Photonics Review*, vol. 13, no. 11, pp. 1–32, Oct. 2019.
[14] A. Zhou, J. Yang, B. Liu, and L. Yuan, "A fiber-optic liquid sensor for simultaneously measuring refractive index, surface tension, contact angle and viscosity," in 2009 20th Int. Conf. Opt. Fibre Sensors, pp. 1–4.
[15] V. A. Márquez-Cruz and J. A. Hernández-Cordero, "Fiber optic Fabry-Perot sensor for surface tension analysis," *Optical Express*, vol. 22, no. 3, p. 3028–3038, Feb. 2014.
[16] C. Shen, C. Zhong, D. Liu, et al., "Measurements of milli-Newton surface tension forces with tilted fiber Bragg gratings," *Optics Letters*, vol. 43, no. 2, p. 255–258, Jan. 2018.
[17] Z. Liu. C. Shen, Y. Xiao, et al., "Liquid surface tension and refractive index sensor based on a tilted fiber Bragg grating," *Journal of the Optical Society of America B*, vol. 35, no. 6, pp. 1282–1287, Jun. 2018.
[18] R. S. Hebbar, A. M. Isloor, and A. F. Ismail, "Contact angle measurements," in Membrane Characterization, 1st ed., N. Hilal, Ed. India, 2017, pp. 219–255.
[19] Y. Tang and S. Cheng, "The meniscus on the outside of a circular cylinder: From microscopic to macroscopic scales," *Journal of Colloid and Interface Science*, vol. 533, pp. 401–408, Aug. 2018.

[20] B. B. Sauer and W. G. Kampert, "Influence of Viscosity on Forced and Spontaneous Spreading : Wilhelmy Fiber Studies Including Practical Methods for Rapid Viscosity Measurement," *Journal Of Colloid And Interface Science*, vol. 37, no. 199, pp. 28–37, Nov. 1998.

[21] S. Yin, and P. Ruffin, "Fiber Optic Sensors," in *Wiley Encyclopedia of Biomedical Engineering.*Hoboken, Ed. New York: Wiley, 2006, pp. 1–8.

[22] C. G. De Mendonça, C. G. Raetano, and C. G. De Mendonça, "Surface tension of mineral oils and vegetable oils," *Engenharia Agricola*, vol. 27, pp. 16–23, Jan. 2007.

[23] J. Kalová and R. Mareš, "Reference values of surface tension of water," *International Journal Thermophysics*, vol. 36, no. 7, pp. 1396–1404, May 2015.

[24] S. Mondal, M.Phukan, A. Ghatak, "Estimation of solid-liquid interfacial tension using curved surface of a soft solid," *Proceedings of the National Academy of Sciences of the United States of America*, vol. 112, no. 41, pp. 12563–12568, Sep. 2015.

[25] S. Richard C. Selley, "The reservoir," in Elements of Petroleum Geology, 3rd ed. vol. 4,M. Geodesy, Ed. United States, 2015, pp. 255–320.

[26] D. A. White and J. A. Tallmadge, "Static menisci on the outside of cylinders," *Journal of Fluid Mechanics.*, vol. 23, no. 2, pp. 325–335, Oct. 1965.

[27] A. Skłodowska, M. Woźniak, and R. Matlakowska, "The method of contact angle measurements and estimation of work of adhesion in bioleaching of metals," *Biological Procedures Online*, vol. 1, no. 3, pp. 114–121, Apr. 1999.

[28] H. Liu and G. Cao, "Effectiveness of the Young-Laplace equation at nanoscale," *Scientific Reports*, vol. 6, pp. 1–10, Apr. 2016.

[29] S. Ehrig et al., "Surface tension determines tissue shape and growth kinetics," *Science Advances*, vol. 5, no. 9, pp. 0–12, Oct. 2019.

[30] N. Wu, X. Li, S. Liu, M. Zhang, and S. Ouyang, "Effect of hydrogen bonding on the surface tension properties of binary mixture (acetone-water) by Raman spectroscopy," *Applied Science*, vol. 9, no. 6, pp. 2–10, Mar. 2019.

[31] R. Bonhomme, J. Magnaudet, F. Duval, and B. Piar, "Inertial dynamics of air bubbles crossing a horizontal fluid-fluid interface," *Journal of Fluid Mechanics*, vol. 707, pp. 405–443, Sep. 2012.